Quantitative tracking of tumor cells in phase-contrast microscopy exploiting halo artifact pattern

Mi-Sun Kang[a], Soo-Min Song[a], Hana Lee[b], Myoung-Hee Kim*[a]
[a]Dept. of Computer Science and Engineering, Ewha Womans University, Seoul, Korea 120750
[b]Dept. of Electronics Engineering, Ewha Womans University, Seoul, Korea 120750

ABSTRACT

Tumor cell morphology is closely related to its invasiveness characteristics and migratory behaviors. An invasive tumor cell has a highly irregular shape, whereas a spherical cell is non-metastatic. Thus, quantitative analysis of cell features is crucial to determine tumor malignancy or to test the efficacy of anticancer treatment. We use phase-contrast microscopy to analyze single cell morphology and to monitor its change because it enables observation of long-term activity of living cells without photobleaching and phototoxicity, which is common in other fluorescence-labeled microscopy. Despite this advantage, there are image-level drawbacks to phase-contrast microscopy, such as local light effect and contrast interference ring, among others.
Thus, we first applied a local filter to compensate for non-uniform illumination. Then, we used intensity distribution information to detect the cell boundary. In phase-contrast microscopy images, the cell normally appears as a dark region surrounded by a bright halo. As the halo artifact around the cell body is minimal and has an asymmetric diffusion pattern, we calculated the cross-sectional plane that intersected the center of each cell and was orthogonal to the first principal axis. Then, we extracted the dark cell region by level set. However, a dense population of cultured cells still rendered single-cell analysis difficult. Finally, we measured roundness and size to classify tumor cells into malignant and benign groups. We validated segmentation accuracy by comparing our findings with manually obtained results.

Keywords: cell morphology, phase-contrast microscopy image, halo artifact, cell classification, cell migration

1. INTRODUCTION

Living cell observation has been widely used by biologists. Computers assist with automatic analysis of microscope images. This automation can improve the screening speed of cancer cell cultures in large data experiments [1].

Previous studies on cell detection have used fluorescence-labeled microscopy, which allows for clearer visualization of object outlines than phase-contrast microscopy does [2,3]. Using confocal or multi-photon microscopy, researchers have attempted to extract 3-dimensional (D) images of cell regions and track changes in these regions. However, phase-contrast microscopy is not often used for this purpose [3] because of the lower image quality obtained. Some studies have proposed that quantitation of cell behavior should be conducted in a 2D environment on cells plated on the bottom of a culture dish and observed using phase-contrast microscopic images [4-7].

We used 3D time-lapse phase-contrast microscopic imaging, which enables long-term observation of live cells. Phase-contrast microscopy is an optical illumination technique in which small phase shifts in the light passing through a specimen are converted into amplitude or contrast changes in the image. The image acquisition process is considerably simpler than that for fluorescent-labeled microscopy, where the object of interest is enhanced using a staining agent. Furthermore, phase-contrast microscopy does not require photobleaching and has no associated phototoxicity, unlike fluorescence microscopy. Thus, it permits cell examination over a long period [2].

The morphology of cells is closely related to their invasiveness and migratory behavior. Invasive tumor cells have a highly irregular shape, whereas non-metastatic cells are spherical. Therefore, quantitative analysis of this feature is crucial to determine tumor invasion and the efficacy of anticancer treatment. This is the most important aspect of analyzing cell morphology and individually migrating cells [8].

mhkim@ewha.ac.kr; phone 82 02 3277-2307

Medical Imaging 2012: Biomedical Applications in Molecular, Structural, and Functional Imaging, edited by Robert C. Molthen, John B. Weaver, Proc. of SPIE Vol. 8317, 83171X · © 2012 SPIE · CCC code: 1605-7422/12/$18
doi: 10.1117/12.911683

In our preliminary study, we used a threshold method to segment cells by halo pattern analysis 9. This method requires images that are more detailed. Thus, we used the advanced active contour method to segment cells. We also propose a 3D cell classification method that is free of image artifacts such as non-uniform illumination and halo patterns. In phase-contrast microscopic images, cells normally appear as dark regions surrounded by a bright halo artifact pattern in the z-depth direction; we identified the cross-sectional plane that intersects each cell through its center and is orthogonal to the first principal axis. We used a histogram-based method to correct for illumination artifacts, extracted the initial cell region by analyzing the intensity, and then segmented the cell region using a level set through the minimization of an energy criterion involving both the region and boundary functions. Finally, we examined the cells' morphology to classify tumor cells as malignant and benign. Fig. 1 is a flowchart of the proposed system.

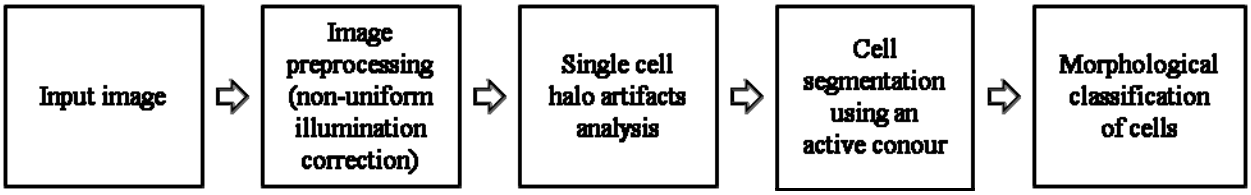

Figure 1. Flowchart of the proposed system.

2. METHODS

In the present study, we used U87, a representative cell line of the rather recalcitrant brain tumor glioblastoma. The images were captured from the same field but at different time points (0, 11, and 25 hours after cell implantation). The magnification was 10×, and we used the Matrigel 3D cell matrix. We developed a Windows-based C++ application program for detection and segmentation. We also trained a support vector machine (SVM) to classify cell morphology.

2.1 Non-uniform illumination correction

Phase-contrast microscopy can be used for living cell analysis and for monitoring cell migration. Phase-contrast microscopy does not require fluorescent labeling. However, because of differences in the light absorption rate, light path, and material properties of cell-culturing gels, the brightness over the image is not uniform. Numerous algorithms have been suggested for brightness correction in image processing and pattern recognition [10]. Gray-scale transformation in the spatial domain, the retinex algorithm, and homomorphic filtering are all commonly used [11-13]. However, it is difficult to select optimal parameter values while considering the characteristics of each image modality. Moreover, this process requires many iterations and a long computation time.

Illumination characteristics can be changed using histogram equalization (HE) by applying the transformation matrix T to the image histogram via global or local approaches. However, image details can be lost in the former, and over-enhancing problems can occur. Locally adapted algorithms divide an image into several sub-blocks and improve the image contrast for each block. Blocking artifacts may appear on section boundaries with this approach.

In the present study, we implemented the localized version of the modification framework histogram-smoothing (MF-HS) algorithm. The MF-HS method enhances the low-dynamic input image without producing over-enhanced artifacts in the resulting image [14,15].

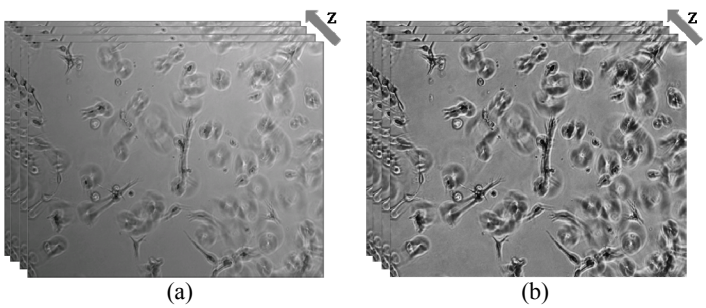

(a) (b)
Figure 2. Contrast-enhancement result sample. (a) Original image, (b) Image after MF-HS–based HE.

2.2 Using the halo pattern to find the cross-sectional plane

A previous study [5] used the intensity profiles obtained during cell image segmentation, such as with 3D object models, for 2D image observation. Oblique cells are oriented in various directions, and the halo pattern around cell borders is difficult to visualize in 2D. Therefore, the current study proposes the cell segmentation method, wherein the orientation and morphology of cells are determined based on 3D information.

In phase-contrast image stacks, cells appear as small bright disks in the focal slice, and they demonstrate growing off-focus phase-contrast interference rings as they move away in the z-stack [2] (Fig. 3). Comparison of the intensity at the center of the cells to that at the cell borders enabled cell body detection [20].

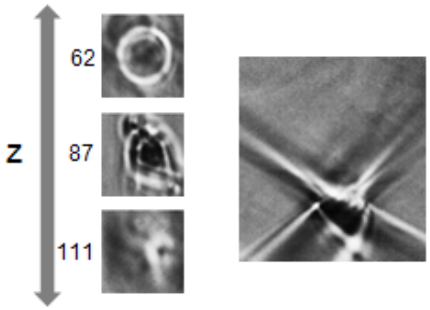

Figure 3. 3D cell appearance correlation. (a) Horizontal slice, (b) Vertical slice

We selected cell image samples for cell detection, calculating the intensity profile and intensity gradient of these samples. We obtained 2 intensity peak values from the center of the cell image (Fig. 4). These peaks refer to the location of the halo artifact around the cell. Thus, we determined a threshold value that was the average threshold range of the samples. The initial region was the threshold of the image obtained after MF-HS–based HE for the detection of cells in an image [16].

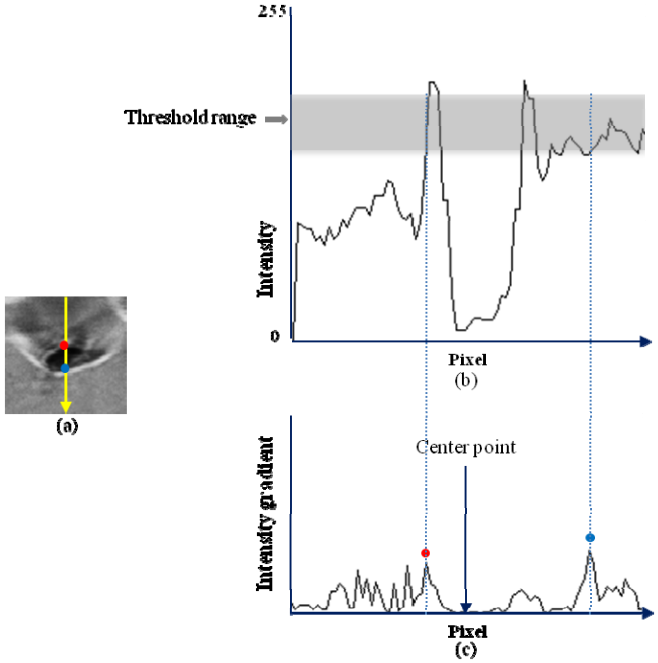

Figure 4. Relationship between the intensity profile of a cell image and Intensity gradient.
(a) Cell image sample (b) Threshold range in the intensity profile at cross-section (c) Intensity gradient at cross-section

We identified the cross-sectional plane that passes through the initial region's center of mass and is orthogonal to the first principal axis (Fig. 5). For this, we used the statistical method of principal component analysis (PCA) [17] to be able to visualize the cells clearly and to ensure less light diffusion and halo artifacts around each cell body [21-22], to estimate the cell objects' rotation, and to understand how each cell lies.

PCA is a widely used mainstay of modern data analysis. It is a simple, non-parametric method of extracting relevant information from complex data sets and has been termed one of the most valuable results of applied linear algebra. It is often used in all forms of analysis, from neuroscience to computer graphics [18]. The rationale behind this approach is that the directions of greatest variability yield the most information about the configuration of the data in multidimensional space. The first principal component will have the greatest variance and yield the largest amount of information from the data [19].

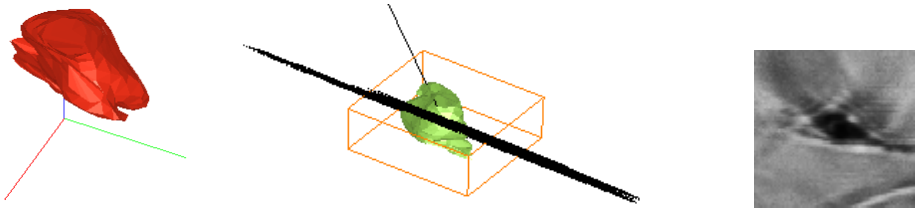

(a) (b) (c)

Figure 5. Initial region sample (a) Initial region of one cell,
(b) The cross-section is orthogonal to the first principle axis, which passes through the center of mass.
(c) Cross-sectional image of sample

2.3 Segmentation

We used the advanced active contour algorithm that was level set to identify the approximate boundary of cells. Level set methods are an important category of modern image-segmentation techniques based on partial differential equations (PDE) [23].

There are 2 types of level set algorithms: fast marching and active contour. The difference among neighboring pixels is evaluated to identify the boundaries of objects. The algorithm is set such that it will converge at the boundary of the object where the differences are high [23].

The fast marching and advanced active contour algorithm is a 2-PDE–based method. Fast marching is akin to a standard flood fill and is sensitive in boundary detection; it calculates the difference of a current selection set of pixel values to that of newly added pixels continuously as the region grows, and stops when it exceeds a preselected gray value difference. This algorithm expands from a seed point to the object boundary until it encounters a pre-set difference in the pixels' intensities. We selected seed points that were the center of mass on individual cells' cross-sectional planes as these points were the center of an initial cell region. Thus, these points were inside the cell region. Fast marching is very similar to flood fill, but with more sophisticated boundary detection.

With regard to the fast marching parameters; first, the gray value difference between boundary pixels and seed point progressively increases and is used to determine the stopping point in expansion. The value will increase with images with stronger contrast. Thus, the value will be decreased for images with no contrast. We set the grey value threshold value as 50. Second, fast marching determines the extent of expansion in one iteration as permitted by selection. It signifies the speed at which the contour progresses; the value is increased to speed up segmentation. Since we selected typical default values, we set the distance threshold value as 0.50.

2.4 Classification

SVMs have recently been found to be powerful classifiers since they are guaranteed to converge to an optimal solution even for a small set of training samples [24]. Therefore, we used SVM-based classification. Once feature vectors were extracted from the segmented cell object, they could be used to analyze the differences in cell size and roundness between benign and malignant cells. We trained a classifier to label new samples into one of these 2 groups.
SVMs can be used to detect statistical differences between 2 populations. In order to acquire the optimal solution, it is important to select a good classifier function. SVMs are known to be robust and free from the problem of over-fitting.

3. EXPERIMENTAL RESULTS

The performance of our segmentation methods is illustrated in Fig. 6. Four images were selected for each cell to test the segmentation methods. The results were compared with the threshold algorithm method that was used previously [9]. The cross-sectional images in Fig. 6 are orthogonal to the first principle axis, which passes through the initial region's center of mass (Figs. 6a, d, g, j), when the threshold method was applied (Figs. 6b, e, h, k), and when we applied our methods (Figs. 6c, f, i, l).

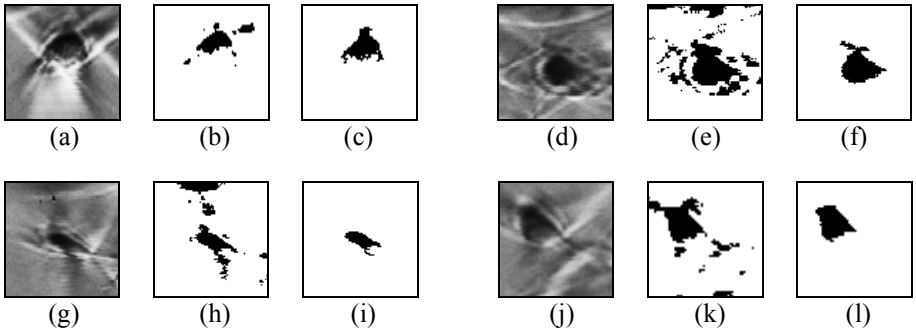

Figure 6. Comparison of threshold segmentation results and results from our method. (a, b, c) Sample 1, (d, e, f) Sample 2, (g, h, i) Sample 3, (j, k, l) Sample 4, (b, e, h, k) Threshold segmentation results, (c, f, i, l) Level set applied results.

We assumed that the cell region would be segmented more clearly with our method than with the method used previously. Threshold algorithm results contain noise that necessitates additional post-processing. We used post-processing to obtain an object in which the morphological opening operation gradually took place, and the spaces representing the cell could be filled in using the morphological closing operation [25].

For experiments with the SVM-based classifier, we collected 2 types of samples (spherical and irregularly shaped) from the segmented images of each cell. We also generated 30 different samples using a training SVM. The features of the training and testing data sets examined were the segmented object's size and roundness. We tested 3 types of kernels: radial-based, polynomial, and sigmoid functions. We adopted the cross-validation technique to overcome the problem associated with the small training sets. We chose the polynomial kernel function, which demonstrated the best classification performance for our data. Fig. 7 illustrates the results of the classification.

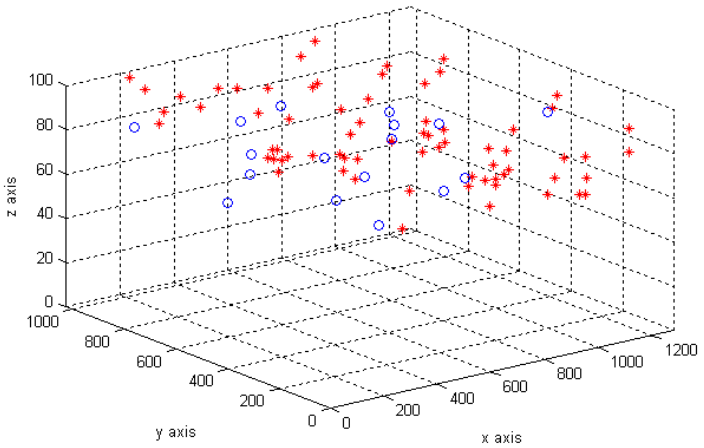

(a) 0 hours

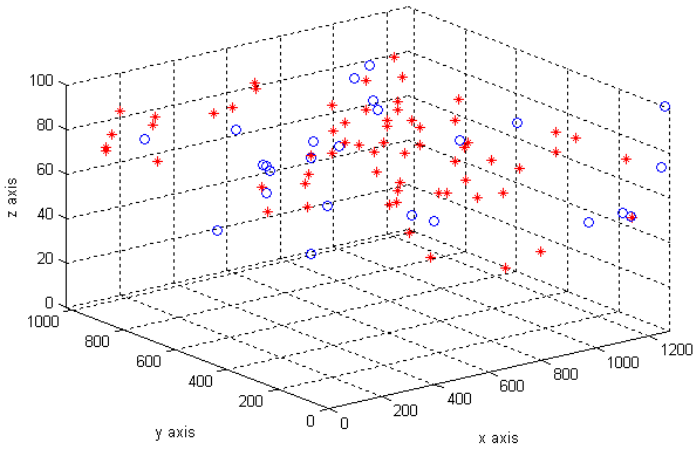

(b) 11hours

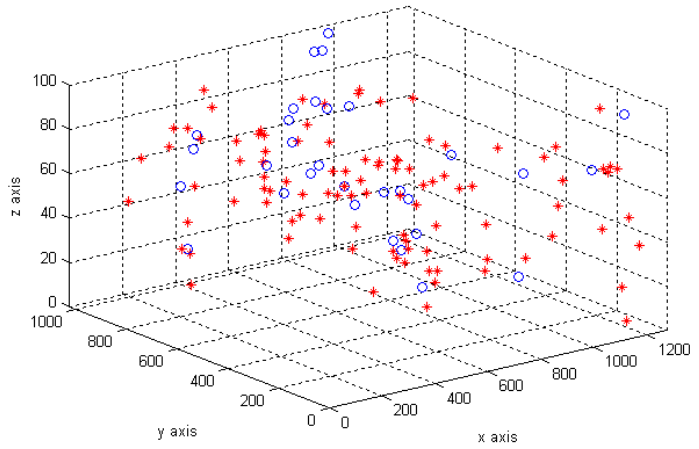

(c) 25 hours

Figure 7. SVM-based classification result. Blue circles represent spherical cells; red stars represent irregular-shaped cells. (a) 0 hours (blue: 18, red: 73), (b) 11 hours (blue: 25, red: 63), (c) 25 hours (blue: 32, red: 99).

We compared the results our method obtained with that obtained manually. Our method provided 84.51% accuracy, while that of the method used previously exceeded 60%. The reason was that the level set algorithm has robust segmentation on thin areas of cell regions from a cell image. Thus, this approach is able to classify tumor cells more clearly than threshold methods are.

4. CONCLUSION

Time-lapse phase-contrast microscopy is becoming increasingly important for studying the invasiveness of tumor cells. We developed a method to detect individual cells in dense cell populations using time-lapse phase-contrast microscopic imaging by taking into consideration the characteristics of imaging modalities and the artifacts in these modalities. We used the level set algorithm by considering the halo artifact on a 3D cross-sectional image. With this approach, we were able to separate cells more clearly than a threshold algorithm could [9]. The results of classification found that cells spread out randomly and that the number of spherical cells was increased [1,8]. We are currently using this method to detect, count, and classify circulating cells based on morphology in time-lapse phase-contrast microscopic images. In the near future, we intend to separate each attached cell, as the current results are of attached cells that were joined together. Furthermore, we intend to develop a system to classify tumor cells as malignant or benign based on morphology, and use our method to screen anticancer drugs.

ACKNOWLEDGEMENTS

This work is financially supported by the Korea Science & Engineering Foundation through the Acceleration Research Program, and by the Ministry of Knowledge Economy (MKE) and Korea Institute for Advancement of Technology (KIAT) through the Human Resource Training Project for Strategic Technology. We thank Dr. Wong of The Methodist Hospital Research Institute for providing time-lapse phase-contrast microscopic images of cell line.

REFERENCES

[1] Decaestecker, C., Debeir, O., Van Ham, P. and Kiss, R., "Can anti-migratory drugs be screened in vitro? A review of 2D and 3D assays for the quantitative analysis of cell migration," Med. Res. Rev., 27, 149-176 (2007).

[2] Li, K., Chen, M., Kanade, T., Miller, E. D., Weiss, L. E. and Campbell, P. G., "Cell population tracking and lineage construction with spatiotemporal context," Med. Image Anal., 12(5), 546-566 (2008).

[3] Adanja, I., Debeir, O., Megalizzi, V., Kiss, R., Warzee, N. and Decaestecker, C., "Automated tracking of unmarked cells migrating in three-dimensional matrices applied to anti-cancer drug screening," Exp. Cell Res., 316, 181-193 (2010).

[4] Pan, J., Kanade, T. and Chen, M., "Learning to detect different types of cells under phase contrast microscopy," Proc. MIAAB (2009).

[5] Magg, M., "Tracking cells in phase contrast light microscopic images," Diploma Theses (2010).

[6] Orikawa, J. and Tanaka, T., "Cell segmentation from phase-contrast images using hybrid watershed and region growing algorithm for genomic drug discovery," Proc. SICE (2011).

[7] Hadjidemetriou, S., Gabrielli, B., Pike, T., Stevens, F., Mele, K. and Vallotton, P., "Detection and tracking of cell divisions in phase contrast video microscopy," Proc. MIAAB (2008).

[8] Friedl, P., Zanker, K. S., and Brocker, E. B., "Cell migration strategies in 3D extracellular matrix: differences in morphology, cell matrix interactions, and integrin function," Microsc. Res. Tech., 43, 369-378 (1998).

[9] Kang, M. S., Song, S. M., Lee, H. A. and Kim, M. H., "Cell morphology classification in phase contrast microscopy image reducing halo artifact," Proc. SPIE, (2012).

[10] Vovk, U., Pernus, F. and Likar, B., "A review of methods for correction of intensity inhomogeneity in MRI," IEEE Trans. Med. Imaging, 26(3), 405-421 (2007). s

[11] Gonzales, R. C. and Wintz, P., [Digital Image Processing], Addison-Wesley (1987).

[12] Jobson, D. J., "A multiscale retinex for bridging the gap between color images and the human observation of scenes," IEEE Trans. Image Process., 6(7), 965-976 (1997).

[13] Stockham, T. G., "Image processing in the context of a visual model," Proc. IEEE, 60(7), 828-842 (1972).

[14] Lee, H. A., Kim, J. S., Kim, J. T. and Kim, M. H., "Histogram based correction of non-uniform illumination on phase-contrast Microscopy," Proc. IPIU (2010).

[15] Arici, T., Dikbas, S. and Altunbasck, Y., "A histogram modification framework and its application for image contrast enhancement," IEEE Trans. Image Process., 15, 1921-1935 (2009).

[16] Prewitt, J. M. S. and Mendelsohn, M. L., "The analysis of cell images," Ann. N. Y. Acad. Sci., 128, 1035-1053 (1966).

[17] Smith, L., "A Tutorial on Principal Components Analysis," (2002).

[18] Shlens, J., "A tutorial on principal component analysis," (2005).

[19] Kolenikov S. and Angeles, G., "The use of discrete data in PCA: Theory, simulations, and applications to socioeconomic indices," Technical Report, Carolina Population Center, University of North Carolina at Chapel Hill, Oct. 20 (2004).

[20] Bradhurst, C. J., Bokes, W. and Xiao, Y., "Segmentation of bone marrow stromal cells in phase contrast microscopy images," Proc. IVCN, 1-6 (2008).

[21] Watanabe, Y., "A method for volume estimation by using vector areas and centroids of serial cross sections," IEEE Trans. Biomed. Eng. 29(3), 202-205 (1982).

[22] Treece, G. M., "Volume Measurement and Surface Visualisation in Sequential Freehand 3D Ultrasound," Ph.D. Thesis, Cambridge University (2000).

[23] Yoo, T. S., [Insight into Images: Principles and Practice for Segmentation, Registration, and Image Analysis], CRC Press (2004).

[24] Vapnik, V. N., [The Nature of Statistical Learning Theory], Springer (1995).

[25] Anoraganingrum, D., "Cell segmentation with median filter and mathematical morphology operation," Proc. ICIP, 1043-1046 (1999).

REFERENCE LINKING

book:

[11] Gonzales, R. C. and Wintz, P., [Digital Image Processing], Addison-Wesley (1987).

[23] Yoo, T. S., [Insight into Images: Principles and Practice for Segmentation, Registration, and Image Analysis], CRC Press (2004).

[24] Vapnik, V. N., [The Nature of Statistical Learning Theory], Springer, (1995).

journal paper:

[1] Decaestecker, C., Debeir, O., Van Ham, P. and Kiss, R., "Can anti-migratory drugs be screened in vitro? A review of 2D and 3D assays for the quantitative analysis of cell migration," Med. Res. Rev., 27, 149-176 (2007).

[2] Li, K., Chen, M., Kanade, T., Miller, E. D., Weiss, L. E. and Campbell, P. G., "Cell population tracking and lineage construction with spatiotemporal context," Med. Image Anal., 12(5), 546-566 (2008).

[3] Adanja, I., Debeir, O., Megalizzi, V., Kiss, R., Warzee, N. and Decaestecker, C., "Automated tracking of unmarked cells migrating in three-dimensional matrices applied to anti-cancer drug screening," Exp. Cell Res., 316, 181-193 (2010).

[8] Friedl, P., Zanker, K. S., and Brocker, E. B., "Cell migration strategies in 3D extracellular matrix: differences in morphology, cell matrix interactions, and integrin function," Microsc. Res. Tech., 43, 369-378 (1998).

[10] Vovk, U., Pernus, F. and Likar, B., "A review of methods for correction of intensity inhomogeneity in MRI," IEEE Trans. Med. Imaging, 26(3), 405-421 (2007).

[12] Jobson, D. J., "A multiscale retinex for bridging the gap between color images and the human observation of scenes," IEEE Trans. Image Process., 6(7), 965-976 (1997).

[15] Arici, T., Dikbas, S. and Altunbasck Y., "A histogram modification framework and its application for image contrast enhancement," IEEE Trans, Image Process, 15, 1921-1935 (2009).

[16] Prewitt, J. M. S. and Mendelsohn, M. L., "The analysis of cell images," Ann. N. Y. Acad. Sci., 128, 1035-1053 (1966).

[21] Watanabe, Y., "A method for volume estimation by using vector areas and centroids of serial cross sections," IEEE Trans. Biomed. Eng., 29(3), 202-205 (1982).

proceedings paper:

[4] Pan, J., Kanade, T. and Chen, M., "Learning to detect different types of cells under phase contrast microscopy," Proc. MIAAB (2009).

[6] Orikawa, J. and Tanaka, T., "Cell segmentation from phase-contrast images using hybrid watershed and region growing algorithm for genomic drug discovery," Proc. SICE (2011).

[7] Hadjidemetriou, S., Gabrielli, B., Pike, T., Stevens, F., Mele, K. and Vallotton, P., "Detection and tracking of cell divisions in phase contrast video microscopy," Proc. MIAAB (2008).

[9] Kang, M. S., Song, S. M., Lee, H. A. and Kim, M. H., “Cell morphology classification in phase contrast microscopy image reducing halo artifact,” Proc. SPIE, (2012).

[13] Stockham, T. G., “Image processing in the context of a visual model,” Proc. IEEE, 60(7), 828-842 (1972).

[14] Lee, H. A., Kim, J. S., Kim, J. T. and Kim, M. H., “Histogram based correction of non-uniform illumination on phase-contrast microscopy,” Proc. IPIU (2010).

[20] Bradhurst, C. J., Bokes, W. and Xiao, Y., “Segmentation of bone marrow stromal cells in phase contrast microscopy images,” Proc. IVCN, 1-6, (2008).

[25] Anoraganingrum, D., “Cell segmentation with median filter and mathematical morphology operation,” Proc. ICIP, 1043-1046, (1999).